Neurobiology of Disease

Mutant Huntingtin Inhibits αB-Crystallin Expression and Impairs Exosome Secretion from Astrocytes

Yan Hong, Ting Zhao, Xiao-Jiang Li, and Shihua Li
Department of Human Genetics, Emory University School of Medicine, Atlanta, Georgia 30322

In the brain, astrocytes secrete diverse substances that regulate neuronal function and viability. Exosomes, which are vesicles produced through the formation of multivesicular bodies and their subsequent fusion with the plasma membrane, are also released from astrocytes via exocytotic secretion. Astrocytic exosomes carry heat shock proteins that can reduce the cellular toxicity of misfolded proteins and prevent neurodegeneration. Although mutant huntingtin (mHtt) affects multiple functions of astrocytes, it remains unknown whether mHtt impairs the production of exosomes from astrocytes. We found that mHtt is not present in astrocytic exosomes, but can decrease exosome secretion from astrocytes in HD140Q knock-in (KI) mice. N-terminal mHtt accumulates in the nuclei and forms aggregates, causing decreased secretion of exosomes from cultured astrocytes. Consistently, there is a significant decrease in secreted exosomes in both female and male HD KI mouse striatum in which abundant nuclear mHtt aggregates are present. Conversely, injection of astrocytic exosomes into the striatum of HD140Q KI mice reduces the density of mHtt aggregates. Further, mHtt in astrocytes decreased the expression of αB-crystallin, a small heat shock protein that is enriched in astrocytes and mediates exosome secretion, by reducing the association of Sp1 with the enhancer of the *αB-crystallin* gene. Importantly, overexpression of αB-crystallin rescues defective exosome release from HD astrocytes as well as mHtt aggregates in the striatum of HD140Q KI mice. Our results demonstrate that mHtt reduces the expression of αB-crystallin in astrocytes to decrease exosome secretion in the HD brains, contributing to non–cell-autonomous neurotoxicity in HD.

Key words: αB-crystallin; astrocytes; exosome; Huntington disease; release

Significance Statement

Huntington's disease (HD) is characterized by selective neurodegeneration that preferentially occurs in the striatal medium spiny neurons. Recent studies in different HD mouse models demonstrated that dysfunction of astrocytes, a major type of glial cell, leads to neuronal vulnerability. Emerging evidence shows that exosomes secreted from astrocytes contain neuroprotective cargoes that could support the survival of neighboring neurons. We found that mHtt in astrocytes impairs exosome secretion by decreasing αB-crystallin, a protein that is expressed mainly in glial cells and mediates exosome secretion. Overexpression of αB-crystallin could alleviate the deficient exosome release and neuropathology in HD mice. Our results revealed a new pathological pathway that affects the critical support of glial cells to neurons in the HD brain.

Introduction

Huntington's disease (HD) is a fatal, autosomal-dominant, inherited neurodegenerative disorder that is caused by an expanded polyglutamine repeat in the N-terminal region of huntingtin (Ross and Tabrizi, 2011; Bates et al., 2015). Although neuronal cells are preferentially degenerated in HD, the function of glial cells is also affected by mutant huntingtin (mHtt) (Hsiao and Chern, 2010; Lee et al., 2013). For example, mHtt reduces expression levels of EAAT2 (GLT-1) and potassium ion channel (Kir4.1) in astrocytes, which consequently increases neuronal excitotoxicity (Shin et al., 2005; Bradford et al., 2009; Tong et al., 2014). Our recent studies show that mHtt also decreases BDNF secretion by compromising exocytosis of dense-core vesicles in astrocytes (Hong et al., 2016). These findings suggest that mHtt may impair multiple functions in astrocytes.

Recent studies found that astrocytes also secrete exosomes to support the normal function and survival of neuronal cells (Taylor et al., 2007; Guitart et al., 2016). Exosomes are small membra-

Received May 23, 2017; revised Aug. 23, 2017; accepted Aug. 25, 2017.

Author contributions: Y.H., X.-J.L., and S.L. designed research; Y.H. and T.Z. performed research; Y.H. and T.Z. contributed unpublished reagents/analytic tools; Y.H., X.-J.L., and S.L. analyzed data; Y.H., X.-J.L., and S.L. wrote the paper.

This work was supported by National Institutes of Health NS036232 and NS101701 to X.-J.L., and Grants NS095279 and NS095181 to S.L. We thank the Integrated Cellular Imaging Core at Emory University for the use of imaging facilities.

The authors declare no competing financial interests.

Correspondence should be addressed to either Dr. Shihua Li or Dr. Xiao-Jiang Li, Department of Human Genetics, Emory University School of Medicine, 615 Michael Street, Atlanta, GA 30322. E-mail: sli@emory.edu or xli2@emory.edu.

DOI:10.1523/JNEUROSCI.1418-17.2017

 0270-6474/17/379550-14$15.00/0

nous vesicles (40–100 nm) secreted by multiple cell types and can be isolated from conditioned cell culture media or body fluids. Functions of exosomes include exchanging signals with neighboring cells, removing unwanted proteins, and transfer of pathogens between cells. Exosomes contain different types of mRNA, miRNA, and proteins, which are dependent on the host cells that produce exosomes (Théry, 2011; Jarmalavičiūtė and Pivoriūnas, 2016). Exosomes from neuronal cells can spread misfolded proteins between cells, a mechanism underlying the spread of toxic proteins in the brain (Bellingham et al., 2012; Wang et al., 2017). However, exosomes from glial cells can carry neuroprotective molecules to prevent neuron degeneration (Hajrasouliha et al., 2013; Haney et al., 2013; Zhao et al., 2014; Guitart et al., 2016; Xin et al., 2017). Astrocyte-derived exosomes carry neuroprotective cargoes, such as Hsp70 and HspB1, to execute neuroprotective function (Taylor et al., 2007; Nafar et al., 2016). Whether mHtt is present in astrocytic exosomes to spread mHtt or affects astrocytic exosome biogenesis, release, or both remains unknown.

Using primary astrocyte cultures from the HD 140Q knock-in (KI) mouse model that express full-length mHtt at the endogenous level, we found that mHtt is undetectable in astrocyte-derived exosomes, suggesting that mHtt is not transferred by astrocytic exosomes. Instead, the secretion of exosomes from HD astrocytes is affected. αB-crystallin is a small heat shock protein that is enriched in astrocytes as well as oligodendrocytes and mediates exosome secretion (Gangalum et al., 2016). We found that αB-crystallin is deficient in HD astrocytes because mHtt affects its transcription. More importantly, overexpression of αB-crystallin improved exosome secretion from HD astrocytes and ameliorated the neuropathology in HD KI mice. Our findings demonstrate, for the first time, that mHtt impairs exosome secretion by astrocytes, and suggest a new mechanism underlying non–cell-autonomous neurotoxicity of mHtt.

Materials and Methods

Animals. Full-length Htt 140Q KI mice (Hickey et al., 2008) were maintained at the Emory University Animal facility. Both male and female pups from these mice were used for primary cultures. Male and female adult mice at different ages were used for viral injection and brain tissue isolation. This study strictly followed the recommendations in the National Institutes of Health *Guide for the care and use of laboratory animals*. The protocol was approved by the Committee on the Ethics of Animal Experiments of Emory University (Permit 2002557).

Antibodies and reagents. Primary antibodies included anti-expanded polyQ (1C2) (Millipore, MAB1574), anti-Htt (mEM48), anti-V5 (Invitrogen, 46-0705), anti-GFAP (Millipore, MAB360), anti-NeuN (Millipore, ABN78), anti-Alix (Millipore, ABC40), anti-flotillin-1 (Millipore, MAB1118), anti-αB-crystallin (Abcam, ab13496), anti-Hsc70 (Santa Cruz Biotechnology, sc7298), anti-Hsp90 (Cell Signaling Technology, 4874S), anti-GAPDH (Millipore Bioscience Research Reagents, MAB374), anti-GM130 (BD Biosciences, 610822), anti-GRP78 (Santa Cruz Biotechnology, sc-1051), and anti-CD9 (GeneTex, GTX80172). Secondary antibodies included HRP-labeled donkey anti-mouse, donkey anti-rabbit, donkey anti-mouse AlexaFluor-488 or -594, and donkey anti-rabbit AlexaFluor-488 or -594 from Jackson ImmunoResearch Laboratories. The proteinase inhibitor mixture came from Sigma. The αB-crystallin adenovirus came from SignaGen Laboratories (SL170680), and the Chromatin Immunoprecipitation (ChIP) Assay kit came from Millipore.

Primary cell cultures. Brains from postnatal (day 1–3) murine pups were the source for cultured cortical astrocytes. Following dissection, the cortex was digested with 0.3 mg/ml papain. The cell suspension was filtered through 70 μm nylon cell strainers (Fisher Scientific). Shaking the cell suspension removed microglia and oligodendrocytes from cultures at DIV14. The remaining cells were detached with 0.25% trypsin and plated for the following experiments. For cortical neuron cultures, cortical neurons were prepared from postnatal day 0 murine pups and the cortex was digested as above. The cell suspension was filtered through 40 μm nylon cell strainers (Fisher Scientific) to remove debris. Neurons were plated at 1×10^6 on poly-D-lysine-coated 6-well plates and cultured in Neurobasal-A medium supplemented with B27 and glutamine (Invitrogen).

Western blotting. Primary cultures or brain tissues were homogenized in ice-cold NP-40 buffer containing a protease inhibitor mixture (Sigma) and 100 μM PMSF. Samples were boiled in protein loading dye containing SDS/β-mercaptoethanol for 5 min and then separated on 4%–12% polyacrylamide Tris-glycine gels purchased from Invitrogen (catalog #EC60385). Proteins were transferred to a nitrocellulose membrane in Tris-glycine buffer. After blocking, blots were probed overnight with different primary antibodies and secondary antibodies. The Western blots were developed using the ECL Prime Chemiluminescence kit (GE Healthcare).

qRT-PCR. Total RNA was isolated from wild-type (WT) and KI astrocytes. Reverse transcription reactions occurred with 1.5 μg of total RNA using the Superscript III First-Strand Synthesis System (Invitrogen). Each reaction included 1 μl of cDNA, 10 μl SYBR Select Master Mix (Applied Biosystems), and 1 μl of each primer in a 20 μl reaction volume for the thermal cycler (Eppendorf, RealPlex Mastercycler).

Stereotaxic injection. Ten-month-old KI mice were injected with adenoviral αB-crystallin. Heads of the animals were placed and fixed in a Kopf stereotaxic frame (Model 1900) equipped with a digital manipulator and a UMP3–1 Ultra pump. The mice were kept deeply anesthetized as assessed by monitoring pinch withdrawal and respiration rate. Each mouse had 4 μl adenoviral αB-crystallin or adenoviral GFP injections in different sides of the striatum (0.6 mm anterior to bregma, 2.0 mm lateral to the midline, 3.5 mm ventral to dura). The injections occurred at a rate of 0.2 μl/min. The needle was left in place for 10 min after each injection to minimize the upward flow of viral solution. αB-crystallin-V5 expression occurred over 30 d *in vivo* before collecting the brains for further analysis. Exosomes from WT or KI astrocytes culture resuspended in PBS for exosome injection. A total of 8 μl of PBS, WT, or KI astrocytic exosomes were injected into two sites of striatum in one hemisphere (0.6/0.4 mm anterior to bregma, 2.0 mm lateral to the midline, 3.5 mm ventral to dura) in 9-month-old KI mice with 4 μl for each site. PBS injection served as a control. Seven days after injection, the mouse brains were dissected and prepared for immunocytochemistry.

Immunofluorescent staining. Cultured astrocytes were fixed with 4% PFA for 8–10 min. Mouse brains were sectioned at 10 μm thickness using a cryostat at −20°C. Sections were mounted onto gelatin-coated sides and fixed with 4% PFA for 10 min. Fixed sections were blocked with 3% BSA/0.2% Triton X-100 for 30 min at room temperature. Following incubation of fixed sections with primary antibodies and washes at 4°C overnight, fluoro-conjugated secondary antibodies and Hoechst nuclear dye were added to the samples for staining. An Olympus FV1000 inverted microscope with a digital camera system captured astrocyte sample and brain section images. Quantitative analysis of GFAP staining occurred using the method in our previous studies (Hong et al., 2016). Briefly, National Institutes of Health ImageJ software was used to measure GFAP immunostaining intensity. Color images obtained with a 63× objective were converted to 8-bit black-and-white images. The "Threshold" function was used to adjust the background to highlight GFAP-specific staining. The same threshold was applied to all images captured for analysis. Finally, the "Measure" function quantified GFAP staining intensity in each image. Each group had 7–10 images per section and 8 sections per group were examined.

Purification of exosomes. Exosomes were prepared from culture medium as described previously (Théry et al., 2006; Takeuchi et al., 2015; Iguchi et al., 2016; Westergard et al., 2016). Briefly, astrocytes were cultured in 100 mm dish (2×10^6). The astrocyte culture medium was replaced with the culture medium containing 10% exosome-free FBS (EXO-FBS-50A-1, SBI). After 24 h incubation, astrocyte culture medium was transferred to a centrifuge tube and centrifuged sequentially at $300 \times g$ for 10 min, $2000 \times g$ for 10 min, $10{,}000 \times g$ for 30 min, and $100{,}000 \times g$ for 70 min. The pellet was resuspended in cold PBS and centrifuged at $100{,}000 \times g$ for an additional 70 min. The exosome-containing pellet was

resuspended in appropriate buffers. All centrifugations occurred at 4°C. After removing cell culture medium, astrocytes were lysed in NP40 buffer. The purity of exosomes was identified by Western blotting using exosome marker antibodies to Alix, flotillin-1, and HSC70 as described in previous studies (Théry et al., 2006; Takeuchi et al., 2015; Iguchi et al., 2016; Westergard et al., 2016). Western blotting results show that only exosome markers, but not ER and Golgi markers, are present in exosome fraction, indicating the purity of exosomes. The ratio of Alix or flotillin-1 in the exosome fraction to those in the total astrocytes lysates was used to estimate the amount of exosome secreted from WT and KI astrocytes.

Exosomes from mouse brain tissues were prepared as previously described (Perez-Gonzalez et al., 2012; Polanco et al., 2016). In brief, the striatum were dissected from HD KI and age- and gender-matched WT controls. These tissues were chopped before being treated with 20 units/ml papain in Hibernate A solution for 15 min at 37°C. The reaction was stopped with 2 volumes of cold Hibernate A solution containing protease inhibitor mixture. The tissues were gently disrupted by pipetting with a 10 ml pipette, followed by a series of differential centrifugation as described above. The supernatant from the 10,000 × *g* centrifugation step was filtered through a 0.22 μm syringe filter and centrifuged at 100,000 × *g* for 70 min at 4°C to pellet exosomes. The pellet was then solubilized in cold PBS and centrifuged at 100,000 × *g* for 70 min. The washed pellet was resuspended in 2 ml of 0.95 M sucrose in 20 mM HEPES, then added to a centrifuge tube containing continuous sucrose gradients (from bottom 2.0, 1.65, 1.3, 0.95, 0.6, to 0.25 M on top, 2 ml each gradient). The continuous sucrose gradients were centrifuged at 200,000 × *g* for 16 h at 4°C. The original six, 2 ml fractions were collected and resuspended in 8 ml ice-cold PBS, followed by 100,000 × *g* centrifugation for 70 min at 4°C. Finally, pellets were resuspended in appropriate buffers. Exosome markers should be mainly present in F3 as shown by Western blotting.

Electron microscopy and immunogold labeling. Exosomes prepared as described above were deposited on collodion-carbon-coated grids and fixed with 2% PFA. The exosomes were permeabilized with 0.1% saponin, followed by immunolabeling with a primary antibody to CD9 and a secondary antibody conjugated with 10 nm gold particles. The exosomes were negatively stained with uranyl acetate for transmission electron microscopy.

ChIP. The ChIP assay, including semiquantitative PCR, was performed as described previously (Bradford et al., 2009). Astrocyte lysates were combined with reagents from the Millipore ChIP Assay kit. After cross-linking, rabbit anti-Sp1 was used to precipitate the Sp1-DNA complex. PCR primers are as follows: forward, 5′AAG ATT CCA GTC CCT GCC CAG 3′; reverse, 5′ TCA CTA GCT CTC TGT CCA CAC C 3′. Proliferating cell nuclear antigen (PCNA) (forward, 5′ TCC TAA GGA TGG AAA CTG CAG CCT 3′; reverse, 5′ ATA GGC GAG GGG CAT CAC GG 3′) was used to amplify the enhancer region of the mouse αB-crystallin gene. PCR amplification with the precipitates from rabbit IgG or absent templates served as negative controls.

Experimental design and statistical analysis. Experiment 1: mHtt is not detectable in exosomes secreted by cultured astrocytes. To investigate whether mHtt is present in the astrocytic exosomes, we isolated exosomes from the culture medium of DIV30 cultured astrocytes isolated from HD 140Q KI mice ($n = 4$ per group). The purity of exosomes was examined by the electron microscopy and Western blotting.

Experiment 2: Astrocytic exosomes have protective effect in HD pathology. To assess the protective effect of exosomes isolated from astrocytes, we injected PBS, purified exosomes from cultured WT or KI astrocytic medium into the striatum of HD KI mice. Both male and female HDKI mice at 9 months old were used for stereotaxic injection ($n = 3$ each group). Seven days after the injection, we performed immunofluorescent staining to examine the mHtt aggregate density in the injected areas. Each group had 8 sections, and 7–10 images per section were examined.

Experiment 3: mHtt reduces exosome secretion from cultured astrocytes. To examine whether mHtt affects the secretion of astrocytic exosomes, we isolated exosomes from DIV30 WT and HD KI astrocyte culture medium and compared the levels of exosome markers (Alix and flotillin-1) by Western blotting. All of the experiments were performed at least three times.

Experiment 4: N-terminal fragments of mHtt impair exosome secretion from cultured astrocytes. To investigate whether exosome secretion from astrocytes is affected by mHtt, we transfected different N-terminal fragments into DIV30 WT astrocytes and compared the levels of exosome markers by Western blotting. $n = 4$ independent experiments of each fragment transfection.

Experiment 5: mHtt decreases exosome secretion from the KI mouse striatum. To investigate whether mHtt affects exosome secretion in the HD KI mouse brain, we isolated exosomes from the cortex and the striatum and compared the levels of exosome markers between WT and KI by Western blotting. Both male and female mice were used for exosome isolation (WT vs KI, $n = 3$/per group). More detailed information can be found in Results (see Fig, 5).

Experiment 6: mHtt impairs αB-crystallin expression both in cultured astrocytes and in the striatum. To examine whether αB-crystallin is decreased in the HD KI mouse model, we performed qPCR and Western blotting to examine the mRNA and protein levels of αB-crystallin used in this experiment. Cultured astrocytes from WT mice served as a control. All of the experiments were performed at least three times. The striatum was isolated from different ages of HD KI mice (3-, 8-, and 10-month-old, $n = 3$/per group).

Experiment 7: Sp1 mediates αB-crystallin expression in astrocytes. To investigate whether mHtt reduces Sp1 occupancy of the αB-crystallin enhancer, we cultured astrocytes at different days (28 and 35 d) and performed CHIP assay to examine whether mHtt reduces the association of Sp1 with the αB-crystallin enhancer in HD KI astrocytes. Cultured astrocytes from WT mice served as a control. PCNA also served as a control. $n = 3$ independent cultures at each age. More detailed information can be found in Results (see Fig, 7).

Experiment 8: αB-crystallin overexpression rescues defective exosome secretion from KI astrocytes. To examine whether overexpression of αB-crystallin can rescue exosome release from HD KI astrocytes, we transfected αB-crystallin-HA plasmid into the cultured KI astrocytes and injected αB-crystallin adenovirus into the striatum of HD KI mice. GFP plasmid, adenoviral-GFP, and adenoviral vector served as controls. Three HD KI mice were injected with each viral vector. We performed Western blotting to compare levels of exosome markers and Immunofluorescent staining to compare mHtt aggregates numbers and reactive astrocytes (GFAP) intensity between control and αB-crystallin overexpression. More detailed information can be found in Results (see Fig. 8).

Statistical analysis. All statistical analyses were performed using Prism (version 6.00, GraphPad Software). All of the experimental data were obtained from at least three independent experiments. Both sexes of mice were used for primary cultures and tissue isolation. Individual statistical analyses are described in detail alongside each experiment in Results. Comparisons of multiple groups were performed using one-way ANOVA followed by *post hoc* tests. Comparisons of two groups were performed using an unpaired two-tailed Student's *t* test. Data are presented as the mean ± SEM, and the significance was set at $p < 0.05$.

Results

mHtt is not detectable in exosomes secreted by cultured astrocytes

Previous research indicates that mHtt may spread from cell to cell (Pecho-Vrieseling et al., 2014; Jeon et al., 2016; Zhang et al., 2016). To examine whether mHtt is a cargo of astrocyte-derived exosomes, we isolated exosomes from the culture medium of primary astrocytes from HD140Q KI mice following the established protocol for exosome isolation (Théry et al., 2006). Briefly, we harvested culture medium of 30-d-old primary astrocytes and centrifuged it at a series of low and high speeds to isolate exosomes (Fig. 1*A*). Transmission electron microscopy of the putative exosome fraction stained with anti-CD9 (an exosome marker) and immunogold labeling showed exosomes of the proper size (40–100 nm) (Fig. 1*B*) in the isolated exosome fraction. Western blotting results showed that additional exosome markers, such as Alix, flotillin-1, and Hsc70, but not Grp78 (ER marker) and GM 130

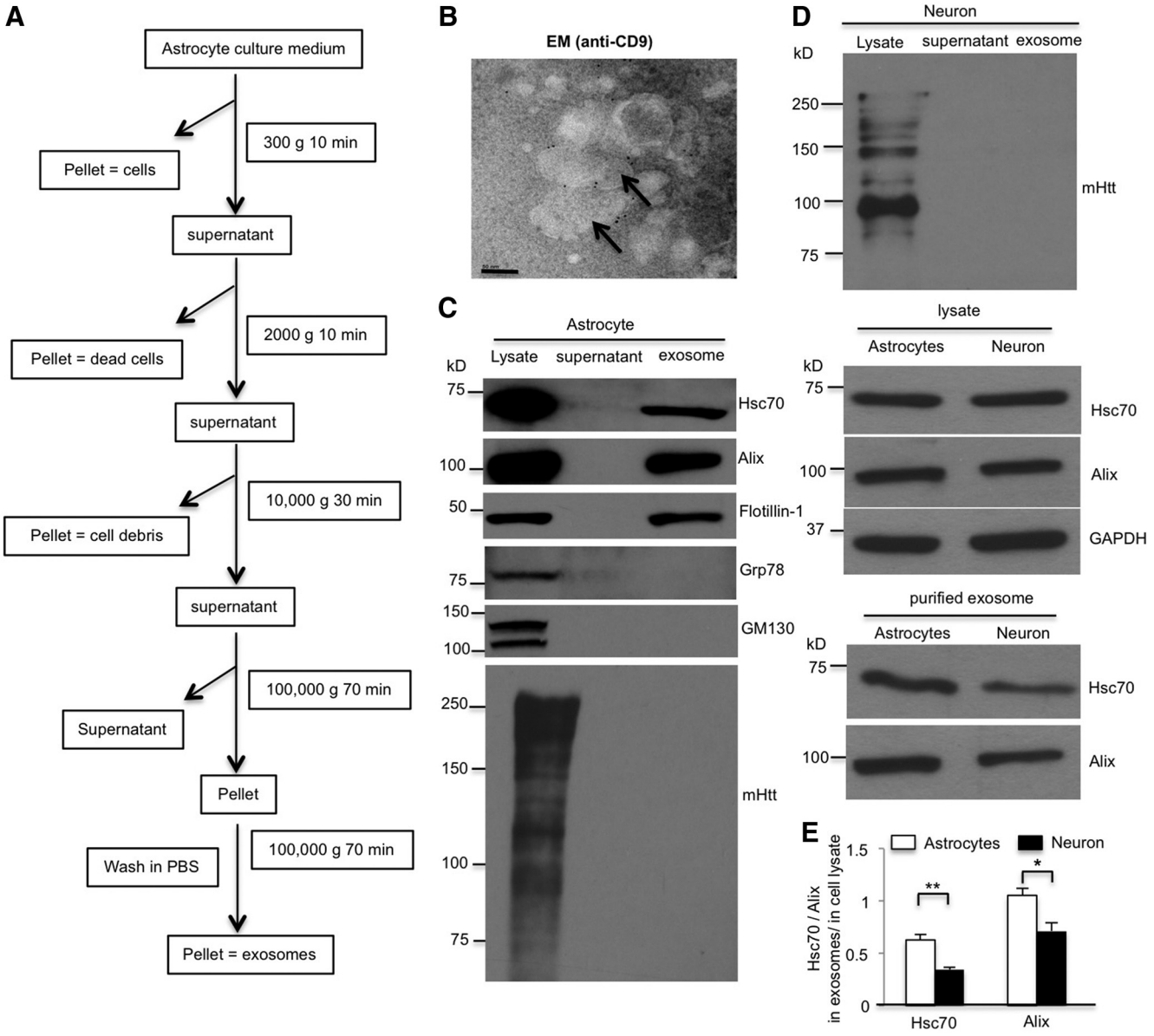

Figure 1. mHtt is not detectable in exosomes secreted by cultured astrocytes. ***A***, Experimental scheme of the exosome purification from astrocyte culture medium. Sequential centrifugations of the culture medium eventually yield the supernatant and exosome pellet fractions. ***B***, Immunoelectron microscopic images of the exosome fraction stained with anti-CD9 antibody and secondary antibody conjugated with 10 nm gold nanoparticles. Scale bars, 50 nm. ***C***, Western blotting analysis of the cellular lysates, supernatant, and exosome fractions using antibodies against the proteins indicated. Alix, flotillin-1, and Hsc70 were detected in the exosome fraction, but Grp78 and GM130 were not. 1C2 immunoblotting revealed that Htt is not found in the astrocytic exosome fraction. ***D***, ***E***, Western blotting with 1C2 antibody showed the absence of Htt in neuronal exosomes. Although Hsc70 and Alix were found at equivalent levels in astrocytic and neuronal lysates, they are more abundant in astrocytic exosomes than in neuronal exosomes (Hsc70, $t = 4.537$, df $= 6$, $p = 0.0039$; Alix, $t = 3.087$, df $= 6$, $p = 0.0215$; Student's t test, $n = 4$ independent cultures). $^{*}p < 0.05$, $^{**}p < 0.01$.

(Golgi marker), are also in the exosome fraction, indicating the purity of exosomes (Fig. 1*C*). Misfolded proteins, such as APP and α-synuclein, associated with certain neurodegenerative disorders, are present in exosomes that are released from neurons (Bieri et al., 2017; Xiao et al., 2017). We also isolated exosomes from cultured HD KI neurons. Interestingly, we did not detect mHtt in the exosomes released from either HD KI astrocytes or neurons (Fig. 1*D*). By comparing exosomes released from astrocytes and neurons having the same quantity of proteins in their lysates, we found that astrocytes secreted more exosomes with more Hsc70 than neurons (Fig. 1*E*). A previous report showed that exosomes isolated from plasma could be injected directly into the mouse brain and then diffused from the injected site (Zheng et al., 2017). To assess the protective effect of exosomes isolated from astrocytes, we injected exosomes isolated from the medium of cultured WT or KI astrocytes into the striatum of HD KI mice. Seven days after the injection, we observed a significant decrease in mHtt aggregate density in the injected areas of WT astrocytic exosomes. We also found that exosomes from KI astrocytes show less effect on Htt aggregates than those from WT astrocytes, supporting the idea that less exosomes were secreted from the KI astrocytes (Fig. 2). It has been demonstrated that exosomes can be taken up by neighboring or distal cells, thus spreading the proteins they carry and subsequently modulating recipient cells (Danzer et al., 2012; Russo et al., 2012). Thus, exosomes secreted by astrocytes carry heat shock proteins, such

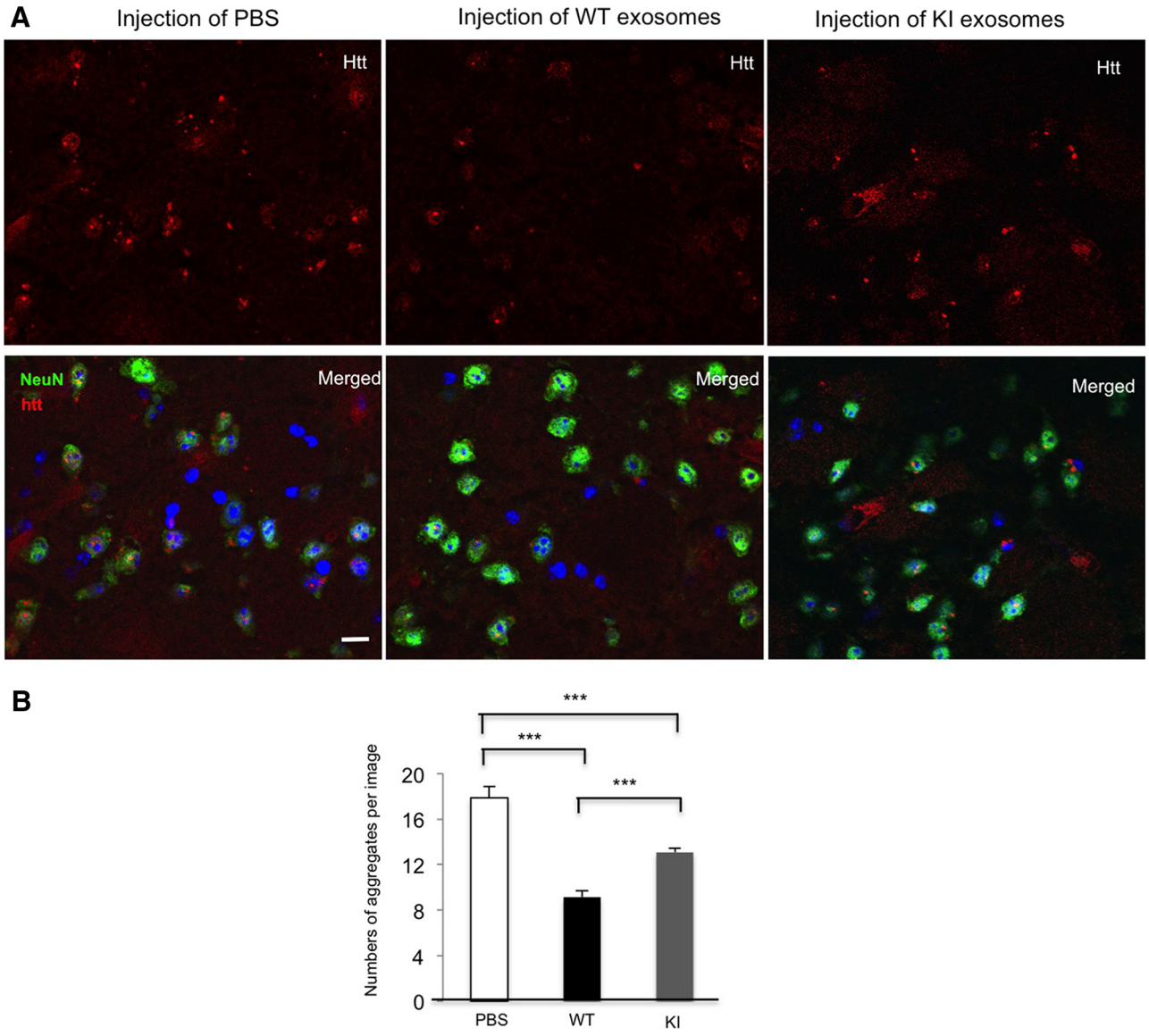

Figure 2. Astrocytic exosomes reduce mHtt aggregate in the striatum of HD KI mice. ***A***, Exosomes were isolated from the culture medium of the same amount (4×10^6 astrocytes) of WT or KI astrocytes and resuspended in PBS. Exosomes from WT or KI astrocytic culture or PBS were injected into the striatum of 9-month-old HD KI mice. Seven days later, the injected striatum was analyzed. High-magnification (63× objective) micrographs showing mHtt aggregates (red), NeuN (green), and nuclei stained by Hoechst (blue) in the striatum of 9-month-old HD KI mice. Scale bars, 5 μm. ***B***, Quantitative analysis shows a significantly decreased number of mHtt aggregates in the site injected with WT astrocytic exosomes compared with the site that was injected with PBS or exosomes from KI mice astrocytes ($F_{(2,177)} = 39.45$, $p < 0.0001$; PBS vs WT, $p < 0.0001$; PBS vs KI, $p < 0.0001$; WT vs KI, $p = 0.0003$; one-way ANOVA followed by Tukey's test, $n = 60$ images from 3 HD KI mice in each group). ***$p < 0.001$.

as Hsc70, Hsp70, and other molecules, which can help appropriate protein folding and promote the degradation of mutant proteins by the ubiquitin-proteasome system in neurons. This finding underscores the significant role of astrocyte-derived exosomes in preventing the accumulation of mHtt in neurons.

mHtt reduces exosome secretion from cultured astrocytes

Given that astrocytic exosomes are protective and that mHtt can impair dense-core vesicles release from astrocyte cultures (Hong et al., 2016), we examined whether mHtt affects the secretion of astrocytic exosomes. Therefore, we isolated exosomes from WT and HD KI astrocyte cell culture medium. Western blotting results showed that two exosome markers, Alix and flotillin-1, are equally present in the lysates of WT and KI astrocytes. However, both Alix and flotillin-1 levels decreased in the isolated exosomes from HD KI astrocytes compared with WT astrocytes (Fig. 3*A*). Quantitative analysis of the ratios of Alix or flotillin-1 in HD KI exosomes to that in WT exosomes showed 59.2% and 34.1% reduction, respectively (Fig. 3*B*). MTS cell proliferation assays indicated that cell viability remained the same in WT and HD KI astrocytes ($n = 4$ independent cultures, WT vs KI, $t = 0.663$, df = 6, $p = 0.532$, Student's t test). These results suggest that mHtt does not affect the biogenesis of exosome proteins but impairs exosome secretion from astrocytes.

N-terminal fragments of mHtt impair exosome secretion from cultured astrocytes

Because small N-terminal mHtt is much more toxic than long mHtt fragments (Davies et al., 1997; Schilling et al., 1999; Slow et al., 2003; Gray et al., 2008), we investigated whether exosome secretion from astrocytes is affected in a fragment length-dependent manner. We transfected different Htt N-terminal fragments (Htt-

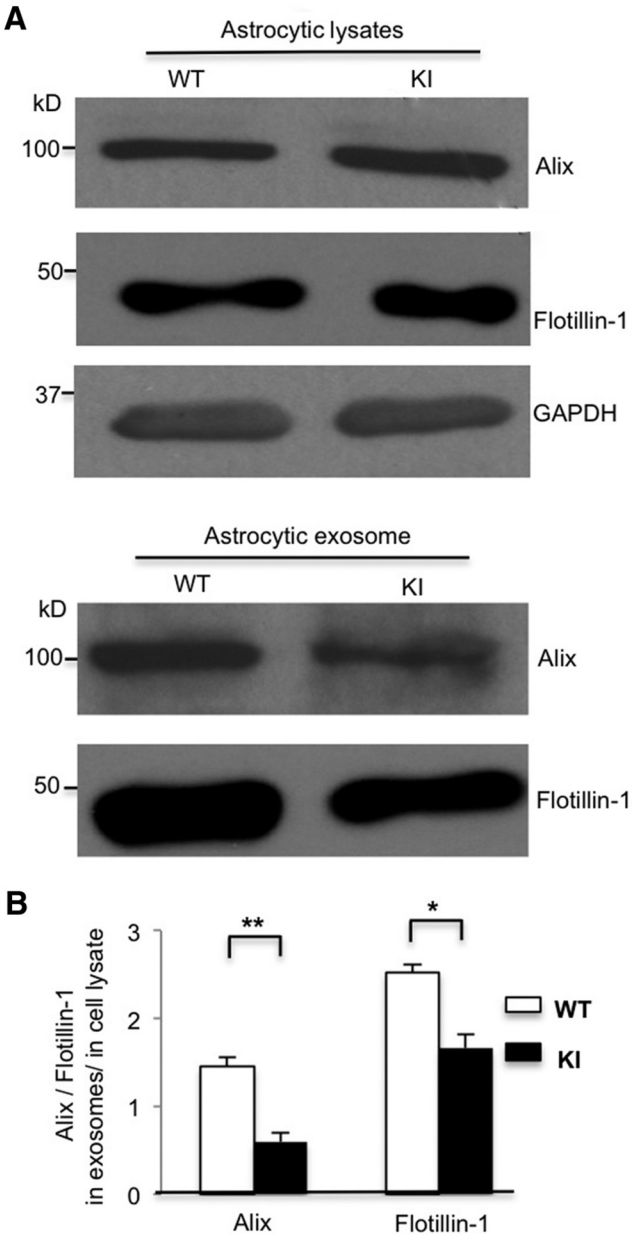

Figure 3. Exosome secretion is decreased from HD KI primary astrocyte cultures. ***A***, Western blot analysis showing the same protein levels of Alix or flotillin-1 in the lysates of WT and HD KI astrocytes, respectively, and decreased Alix and flotillin-1 levels in the exosomes derived from HD KI astrocytes. ***B***, Quantifying ratios of Alix and flotillin-1 levels in exosomes to those in astrocyte lysates (Alix, $t = 5.943$, df $= 4$, $p = 0.004$; flotillin-1, $t = 4.599$, df $= 4$, $p = 0.010$; Student's t test, $n = 3$ independent cultures). $^*p < 0.05$, $^{**}p < 0.01$.

Exon1-20Q, -120Q; Htt-212aa-23Q, -150Q; Htt-508aa-23Q, -120Q) into WT astrocytes (Fig. 4*A*,*B*). Western blotting results showed that, in cell lysates, Alix and flotillin-1 levels are equivalent between WT and mutant N-terminal Htt fragment-transfected astrocytes (Fig. 4*C*,*E*). However, in exosomes derived from astrocytes transfected with other N-terminal Htt fragments, Alix and flotillin-1 levels were significantly reduced when mutant Exon-1 Htt and Htt-212 fragments, but not the longer fragment (Htt-508), were expressed compared with their WT counterparts (Fig. 4*D*,*E*). These results indicate that small N-terminal mHtt fragments were able to inhibit exosome secretion from astrocytes.

mHtt decreases exosome secretion from KI mouse striatum

Next, we wanted to determine whether mHtt affects exosome secretion in the HD KI mouse brain. We isolated exosomes from fresh mouse brain cortical tissues to examine exosome secretion *in vivo*. The fresh cortex tissues were treated with papain to loosen the extracellular matrix and to release extracellular materials (Perez-Gonzalez et al., 2012; Baker et al., 2016; Polanco et al., 2016). The mild papain treatment does not break cell membranes and prevents the contamination of the extracellular fluid with intracellular vesicles. Following a series of low- and high-speed centrifugations, exosomes derived from the cortex were further purified by a sucrose step gradient (Fig. 5*A*). We found that fraction 3 (F3 = 0.95 M sucrose) showed the highest levels of exosome markers, Alix and flotillin-1 (Fig. 5*B*), which is consistent with the previous reports (Perez-Gonzalez et al., 2012; Polanco et al., 2016), indicating that the purified exosomes are in the third fraction in the gradient. We then compared the ratio of Alix and flotillin-1 in F3 with those in the brain tissue lysates from 10-month-old WT and KI mice. Although Alix and flotillin-1 levels were not different in the cortex or striatum lysates from WT and HD KI mice, Alix and flotillin-1 levels were decreased significantly in the exosome fraction isolated from the HD KI striatum, not in the HD KI cortex compared with WT controls (Fig. 5*C*,*D*). In HD KI mice, only the N-terminal mutant Htt forms aggregates, and these aggregates are more abundant in the striatum than the cortex (Li et al., 2000, 2001). Given that mHtt aggregation is a pathological hallmark resulting from the accumulation of misfolded proteins, we examined mHtt aggregation in both astrocytes and neurons. In the double immunofluorescence staining study using antibodies to an astrocytic marker (GFAP) or a neuronal marker (NeuN) and anti-Htt (mEM48), we found the presence of nucleic mHtt aggregates in both astrocytes and neurons in the striatum of 10-month-old HD KI mice (Fig. 5*E*). As reported previously, neuronal aggregates are much larger and more abundant than glial Htt aggregates (Shin et al., 2005; Bradford et al., 2009) because glial cells are able to clear misfolded proteins more efficiently (Tydlacka et al., 2008; Zhao et al., 2016). The presence of aggregated mHtt in astrocytic nuclei supports the idea that mHtt can also accumulate in the nuclei of astrocytes to affect gene transcription (Bradford et al., 2009).

mHtt impairs αB-crystallin expression both in cultured astrocytes and in the striatum

The nuclear localization of mutant Htt in astrocytes led us to investigate whether mHtt affects the transcription of molecules that are important for the release of exosomes. Previous studies show that αB-crystallin, which mediates exosome secretion (Gangalum et al., 2016), is decreased in HD mouse models, such as R6/2 and BACHD mice (Zabel et al., 2002; Oliveira et al., 2016). When comparing the expression of αB-crystallin in cultured astrocytes and neurons, we found that αB-crystallin is much more abundant in astrocytes (Fig. 6*A*). This marked difference led us to examine whether αB-crystallin is also decreased in the HD KI mouse model that expresses full-length Htt at the endogenous level. We used real-time PCR to determine mRNA levels of αB-crystallin in cultured HD KI astrocytes and found that the level of αB-crystallin mRNA does not change at 28 d but decreases at 35 d compared with WT astrocytes (Fig. 6*B*). Consistently, Western blotting revealed that the level of αB-crystallin protein also decreased at 35 d in cultured KI astrocytes compared with WT astrocytes and other heat shock proteins (Fig. 6*C*,*D*). Next, we examined αB-crystallin protein levels in the striatum of HD KI mice to determine whether it is altered during the progression of

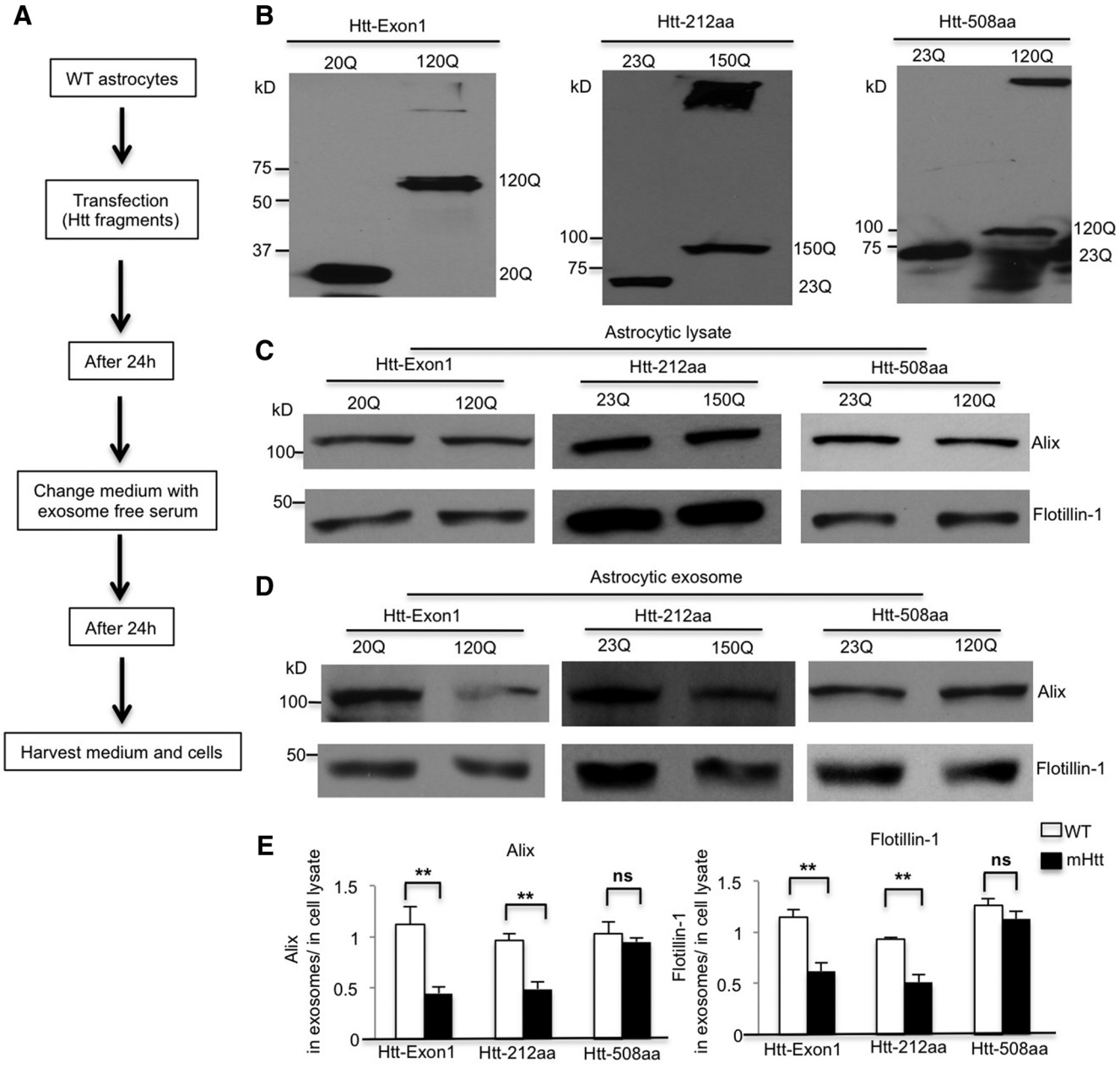

Figure 4. N-terminal fragments of mHtt impair exosome secretion from cultured astrocytes. ***A***, ***B***, Htt fragments, including Exon1 (Htt-Exon1 20Q, 120Q), N-terminal 212 amino acid (Htt-212aa 23Q, 150Q), and N-terminal 508 amino acids (Htt-508aa 23Q, 120Q), were transfected into WT astrocytes. Western blotting with an Htt antibody (mEM48) showed the expression of different Htt fragments in cultured WT astrocytes. ***C***, ***D***, Alix and flotillin-1 protein levels did not change in the lysates of each mutant N-terminal fragment-transfected astrocytes compared with their WT counterparts. However, their levels decreased in exosomes derived from Htt-Exon1-120Q and Htt-212aa-150Q, but not Htt-508aa-120Q transfected astrocytes. ***E***, Quantifying ratios of Alix and flotillin-1 in exosomes to those in astrocytic lysates in each mHtt transfection (Alix, Htt-Exon-1 20Q vs 120Q, $t = 3.809$, df $= 6$, $p = 0.0089$; Htt-212aa 23Q vs 150Q, $t = 4.938$, df $= 6$, $p = 0.0026$; Htt-508aa 23Q vs 120Q, $t = 0.656$ df $= 6$, $p = 0.5366$; flotillin-1, Htt-Exon-1 20Q vs 120Q, $t = 4.884$, df $= 6$, $p = 0.0028$; Htt-212aa 23Q vs 150Q, $t = 5.143$, df $= 6$, $p = 0.0021$; Htt-508aa 23Q vs 120Q, $t = 1.244$, df $= 6$, $p = 0.2599$; Student's *t* test, $n = 4$ independent experiments of each fragment transfection). $^{**}p < 0.01$.

the disease. The striatum was isolated from HD KI mice at different ages (3-, 8-, and 10-month-old) and lysed for Western blotting analysis. αB-Crystallin was not altered until 10 months of age and showed a decrease compared with the WT control after 10 months of age (Fig. 6*E*). The age-dependent decrease in αB-crystallin stays consistent with the age-dependent accumulation of N-terminal Htt fragments and the formation of Htt aggregates in the HD KI mouse striatum.

Sp1 mediates αB-crystallin expression in astrocytes

Although αB-crystallin is decreased in HD mouse brains (Zabel et al., 2002; Oliveira et al., 2016), the mechanism underlying this decrease remains unknown. Because mRNA levels of αB-crystallin are reduced in HD KI astrocytes, we hypothesized that mHtt inhibits αB-crystallin transcription by affecting its promoter activity. Sp1 regulates the activity of αB-crystallin by binding to its enhancer to activate its promoter (Swamynathan et al., 2007). Based on the fact that N-terminal mHtt binds Sp1 in astrocytes and affects the Sp1-dependent transcription of GLT-1 (Bradford et al., 2009), we asked whether mHtt in HD KI astrocytes also reduces Sp1 occupancy of the αB-crystallin enhancer. Because mHtt's accumulation in the nuclei of astrocytes is age-dependent (Shin et al., 2005; Bradford et al., 2009), we performed a ChIP assay using 28-d-old (KI_Y) and 35-d-old (KI_O) astrocyte

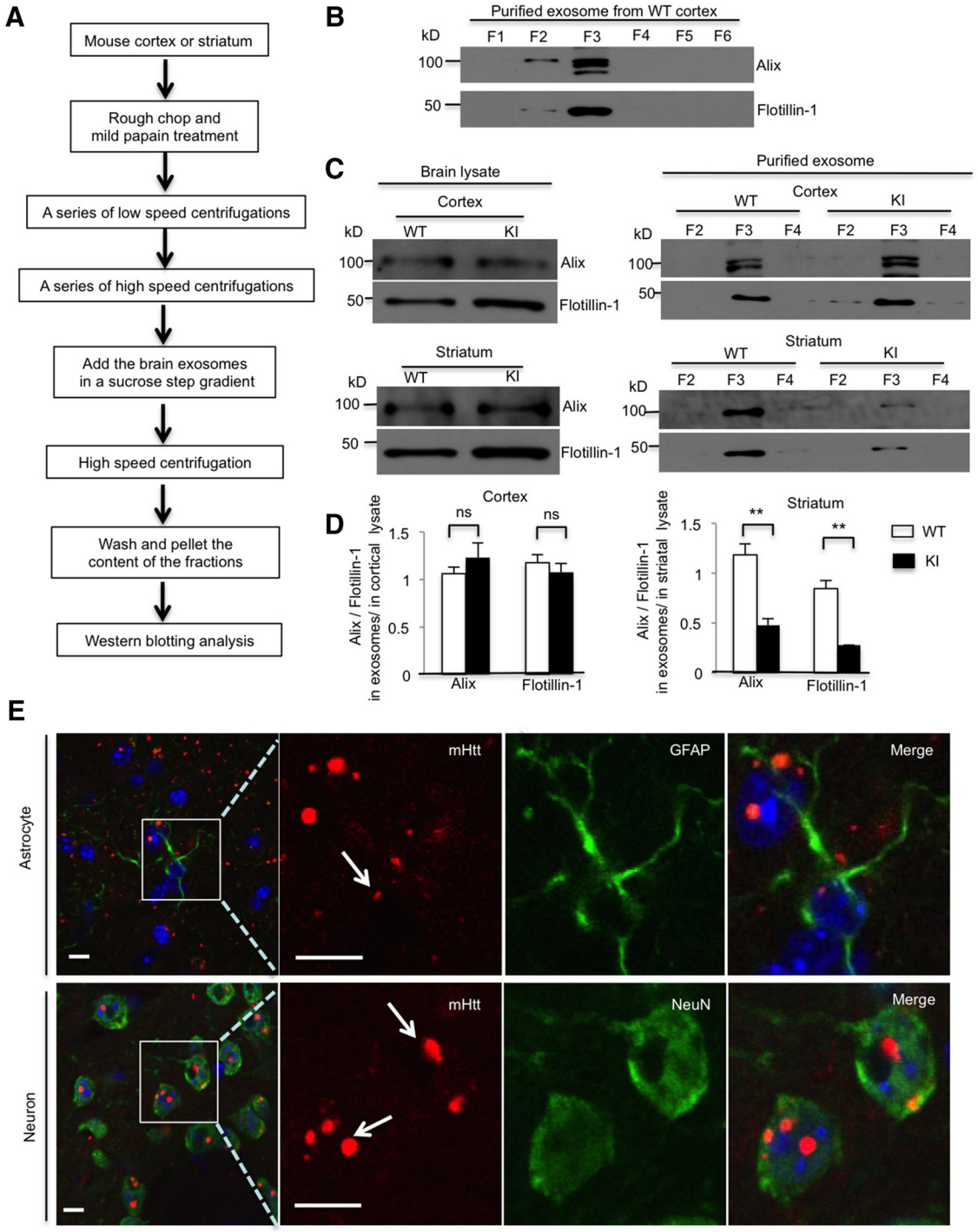

Figure 5. mHtt decreases exosome secretion from HD KI mouse striatum. ***A***, Brain exosome isolation experimental flow chart. ***B***, Western blotting showing that exosome markers, Alix and flotillin-1, are mainly present in F3. ***C***, In the cortex or the striatum, lysates from WT and KI mice, Alix and flotillin-1, were equivalent. However, Alix and flotillin-1 levels significantly decreased in the exosome fraction derived from the HD KI striatum, but not the HD KI cortex compared with WT controls. ***D***, Quantifying ratios of Alix and flotillin-1 in exosomes to those in the cortex or striatal lysates in F3 (cortex, Alix, $t = 1.008$, df $= 4$, $p = 0.3706$; flotillin-1, $t = 0.832$, df $= 4$, $p = 0.452$; striatum, Alix, $t = 5.689$, df $= 4$, $p = 0.0047$; flotillin-1, $t = 6.771$, df $= 4$, $p = 0.0025$; Student's t test, WT and KI, $n = 3$ mice in each genotype). ***E***, Immunostaining showing nuclei mHtt aggregates in both astrocytes and neurons in 10-month-old HD KI striatum. mHtt (red) was probed by 1C2 antibody. GFAP (green, top) indicates astrocytes, and NeuN (green, bottom) indicates neurons. Top, Arrow indicates the small aggregate in the nucleus of astrocyte. Bottom, Arrows indicate the large aggregates in the nuclei of neurons. $^{**}p < 0.01$.

cultures from HD KI mice to examine whether mHtt could reduce the association of Sp1 with the αB-crystallin enhancer in HD KI astrocyte. A greater reduction occurred in the association of Sp1 with the enhancer of αB-crystallin in older (35 d) astrocytes (Fig. 7*A*). However, the association of Sp1 with the αB-crystallin enhancer showed no difference between old (WT_O) and young WT (WT_Y) astrocytes (Fig. 7*A*). These results support the idea that αB-crystallin expression only decreases in the older HD KI astrocytes.

If decreased αB-crystallin levels result from deficient Sp1-mediated transcription in KI astrocytes, then overexpression of Sp1 should rescue decreased αB-crystallin expression and pro-

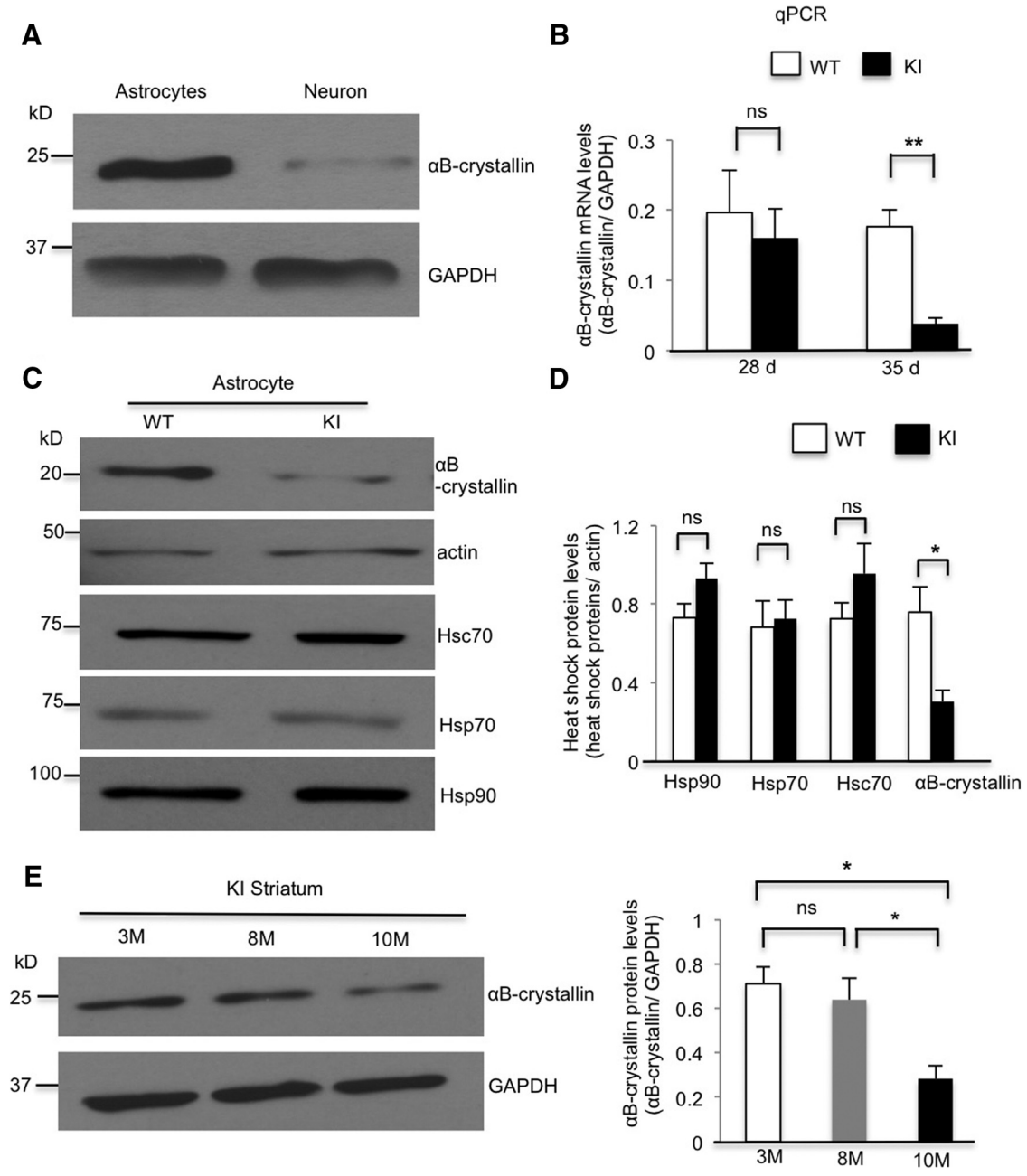

Figure 6. mHtt impairs αB-crystallin expression in both cultured astrocytes and the striatum. ***A***, Western blotting showing that αB-crystallin is enriched in the lysates of cultured astrocytes but deficient in cultured neurons. ***B***, qRT-PCR results revealing a significant reduction in αB-crystallin mRNA in HD KI astrocytes at 35 d of culture, but not at 28 d compared with WT astrocytes (28 d, WT vs KI, $t = 0.484$, df $= 4$, $p = 0.6536$; 35 d, WT vs KI, $t = 5.459$, df $= 4$, $p = 0.0055$; Student's t test, $n = 3$ independent cultures at each age). ***C***, ***D***, Western blotting shows decreased αB-crystallin in cultured HD KI astrocytes at 35 d of culture compared with WT astrocytes. Hsp70, Hsc70, and Hsp90 levels are similar in KI and WT astrocytes (Hsp90, $t = 1.855$, df $= 6$, $p = 0.113$; Hsp70, $t = 0.26$, df $= 4$, $p = 0.807$; Hsc70, $t = 1.33$, df $= 6$, $p = 0.2319$; αB-crystallin, $t = 3.283$, df $= 4$, $p = 0.0304$; Student's t test, $n = 3$ or 4 independent cultures). ***E***, Western blotting showing decreased αB-crystallin levels in the striatum of 10-month-old HD KI mice relative to 3- and 8-month-old KI mice ($F_{(2,6)} = 8.467$, $p = 0.0179$; 3 month vs 8 month, $p = 0.802$; 3 month vs 10 month, $p = 0.02$; 8 month vs 10 month, $p = 0.0427$; one-way ANOVA followed by Tukey's test; $n = 3$ mice at each age). $^*p < 0.05$, $^{**}p < 0.01$.

mote exosome secretion. We then generated an Sp1-HA plasmid to overexpress it in cultured astrocytes. Forty-eight hours after transfection, Western blotting verified that the endogenous αB-crystallin increases by Sp1 overexpression (Fig. 7*B*). Moreover, flotillin-1 increased in the purified exosomes from Sp1-overexpressed KI astrocytes compared with the controls (Fig. 7*C*,*D*). These results suggest that the abnormal association of mHtt with Sp1 can reduce Sp1-mediated αB-crystallin expression, leading to defective exosome secretion from astrocytes.

αB-crystallin overexpression rescues defective exosome secretion from KI astrocytes

Because Sp1 can mediate the expression of a number of genes, it would be important to ask whether direct expression of αB-crystallin can rescue exosome release from HD KI astrocytes. We therefore generated αB-crystallin-HA plasmid to overexpress it in cultured HD KI astrocytes. Forty-eight hours after transfection, Western blotting verified that the expression of αB-crystallin-HA could significantly increase flotillin-1 in the exosome fraction (Fig. 8*A*).

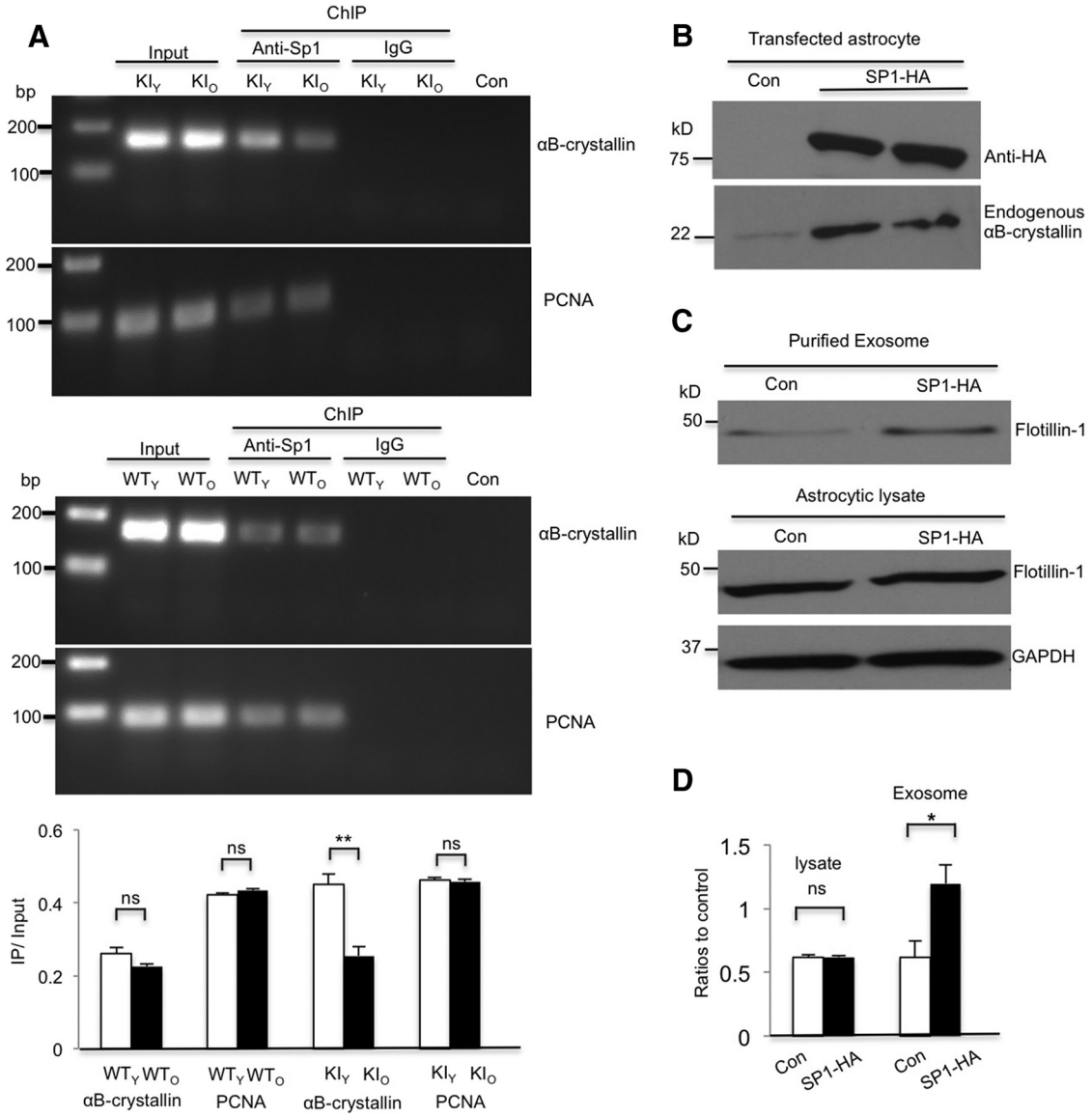

Figure 7. Sp1 mediates αB-crystallin expression in astrocytes. ***A***, ChIP assay results showing decreased association of Sp1 with the αB-crystallin enhancer in 35 d KI (KI_O) astrocytes compared with 28 d KI (KI_Y) astrocytes ($t = 5.346$, df = 4, $p = 0.0059$; Student's t test, $n = 3$ independent cultures at each age). No significant difference between 35 d (WT_O) and 28 d WT (WT_Y) astrocytes was found ($t = 1.921$, df = 4, $p = 0.1272$; Student's t test, $n = 3$ independent cultures at each age). PCNA served as a control (WT_Y vs WT_O, $t = 1.418$, df = 4, $p = 0.2292$; KI_Y vs KI_O, $t = 0.471$, df = 4, $p = 0.662$; Student's t test). Rabbit anti-Sp1 and IgG were used for immunoprecipitation. Con, No template. Quantification of the ratios of PCR products from immunoprecipitated (IP) to input. ***B***, Transfection of mouse Sp1-HA into HD KI astrocytes increased endogenous αB-crystallin expression. ***C***, ***D***, Flotillin-1 levels (flotillin-1/GAPDH) did not change in astrocytic lysates ($t = 0.203$, df = 4, $p = 0.849$; Student's t test) but increased in exosomes (flotillin-1 in exosomes/in cell lysate) derived from Sp1-transfected HD KI astrocytes relative to control plasmid transfection ($t = 2.985$, df = 4, $p = 0.0405$; Student's t test, $n = 3$ independent cultures). *$p < 0.05$.

To confirm the effect of αB-crystallin overexpression *in vivo*, we used αB-crystallin-V5 adenovirus for overexpression in the striatum of HD KI mice via stereotaxic injection. Expression of αB-crystallin-V5 was driven by the CMV promoter, which has high tropism toward astrocytes in the mouse brain (Iino et al., 2001; Yue et al., 2005; Hong et al., 2016). We isolated exosomes from the striatum of HD KI mice 30 d after stereotaxic injection. Western blotting results confirmed the expression of transgenic αB-crystallin with anti-V5 in the striatal lysates (Fig. 8*B*). In these lysates, flotillin-1 was also slightly increased whereas Hsc70 remained unchanged compared with the adenoviral-GFP control. We then purified the exosome fraction and found that both Hsc70 and flotillin-1 significantly increased in exosomes after αB-crystallin overexpression (Fig. 8*C*), suggesting an increase in the released exosomes.

Aggregated Htt appeared as a high MW smear on Western blots and decreased when transgenic αB-crystallin was expressed (Fig. 8*B*). To confirm this, we performed immunofluorescent double staining of the striatum of HD KI mice after injection with an adenoviral vector or adenoviral αB-crystallin. EM48 immunostaining clearly showed a reduction in mHtt aggregates in the αB-crystallin-injected striatum (Fig. 8*D*). In HD KI mouse brains, the increased staining of GFAP reflects reactive astrocytes in the absence of neuronal loss (Yu et al., 2003), which is an early pathology of HD. There was also a reduction of reactive astrocytes by transgenic αB-crystallin (Fig. 8*D*). Quantitative analysis of the density of EM-48-labeled aggregates and GFAP-positive astrocytes confirmed that overexpression of αB-crystallin decreases mHtt aggregates and reactive astrocytes (Fig. 8*E*), which supports the idea that αB-crystallin-mediated exosome secretion protects against HD neuropathology.

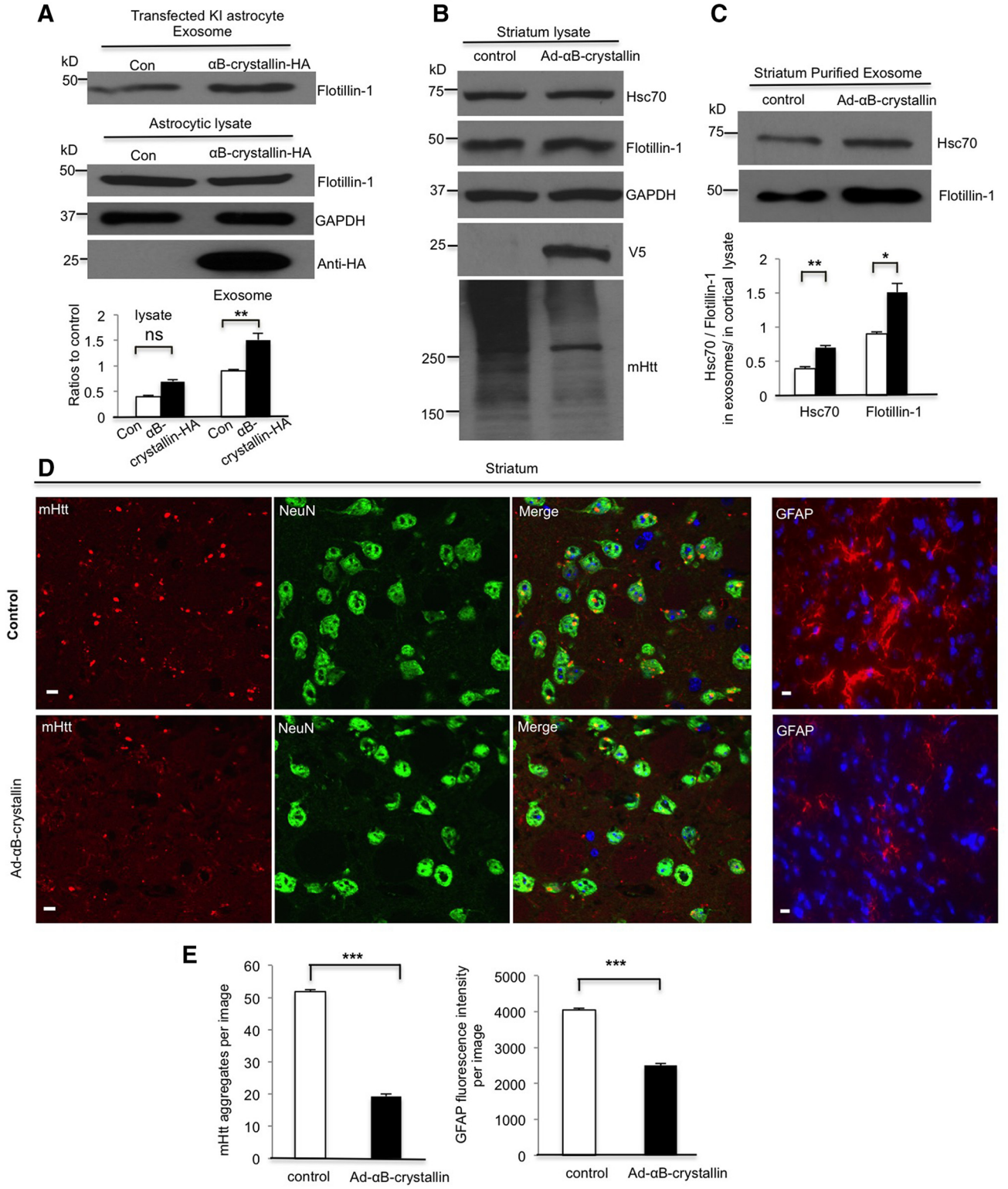

Figure 8. Overexpression of αB-crystallin rescues defective exosome secretion from KI astrocytes. ***A***, Mouse αB-crystallin-HA plasmid was transfected into WT astrocytes. Flotillin-1 (Flotillin-1/GAPDH) remained unchanged in the astrocytic lysate ($t = 0.203$, df $= 4$, $p = 0.1253$ Student's t test, $n = 3$ independent cultures) but increased in exosomes (flotillin-1 in exosomes/in cell lysate) derived from αB-crystallin overexpressed in HD KI astrocytes compared with exosomes from astrocytes that received a control plasmid transfection ($t = 2.985$, df $= 4$, $p = 0.0021$, Student's t test, $n = 3$ independent cultures). ***B***, ***C***, Western blotting verified αB-crystallin-V5 expression *in vivo*. HSC70 and flotillin-1 increased in purified exosomes (Hsc70, $t = 6.548$, df $= 4$, $p = 0.0028$; flotillin-1, $t = 4.503$, df $= 4$, $p = 0.0108$; Student's t test, $n = 3$ αB-crystallin-injected mice), but not in cell lysates from the αB-crystallin-V5-injected striatum compared with an adenoviral-GFP control injection. Levels of mHtt aggregates decreased in the αB-crystallin-V5-injected region. ***D***, High-magnification (63× objective) micrographs showing GFAP staining and mHtt aggregates (red), which are also shown in the merged images with NeuN (green) and nuclei stained by Hoechst (blue), in the striatum of 10-month-old HD mice. Scale bars, 5 μm. ***E***, Quantitative analysis of the GFAP immunofluorescent density showing that GFAP staining and the number of mHtt aggregates significantly decreased in the αB-crystallin-V5-injected striatum compared with the control striatum (mHtt aggregates, control = 51.87 ± 0.53/image vs Ad-αB-crystallin = 19.28 ± 0.67/image, $t = 38.13$, df $= 118$, $p = 3.42621E-68$; GFAP fluorescence intensity, $t = 20.46$, df $= 118$, $p = 1.30096E-40$; Student's t test, $n = 60$ images in each group from 3 HD KI mice). *$p < 0.05$, **$p < 0.01$, ***$p < 0.001$.

Discussion

Exosomes are a type of extracellular vesicles that are secreted from multiple types of cells into biological fluids (Pisitkun et al., 2004; Caby et al., 2005; Vella et al., 2008). Our findings suggest that exosomes secreted from astrocytes are protective against HD pathology. Moreover, mHtt inhibits the release of exosomes from astrocytes, revealing a previously uncovered mechanism for non–cell-autonomous neurotoxicity in HD.

Exosomes can transfer lipids, proteins, and RNAs between cells to play important roles in cell–cell communication under physiological and pathophysiological conditions (Théry et al., 2002; Colombo et al., 2014; Levy, 2017; Maas et al., 2017). Emerging evidence indicates that a number of proteins related to neurodegenerative disorders, including prion disease, Parkinson's disease, and Alzheimer's disease, are present in exosomes and transported by exosomes between cells (Coleman and Hill, 2015). Transfected mutant Htt in cultured cells was also reported to transfer to neighboring cells in culture (Costanzo et al., 2013). In addition, injection of exosomes released from fibroblasts of HD patients into newborn mouse brains triggered the manifestation of an HD phenotype (Jeon et al., 2016). However, it remains unknown whether endogenous exosomes contain mHtt. After examining exosomes isolated from HD KI astrocytes and neurons, we found no evidence for the presence of mHtt in exosomes from these two types of brain cells. It seems that disease proteins are differentially carried by exosomes, and their transport between cells is dependent on the nature of the proteins. Huntingtin is a much larger protein than Tau, α-synuclein, which are smaller and more easily packed into exosomes. Although we could not detect mHtt in exosomes isolated from cultured astrocytes *in vitro*, we cannot rule out the presence of mHtt in astrocytic exosomes in the brain. It is known that, before being released into extracellular space, exosomes are packaged into MVB, whose transport in cells is microtubule-dependent. Because mHtt can compromise microtubule-dependent transport (Saudou and Humbert, 2016), it is possible that mHtt affects exosome secretion from other types of cells, including neurons via a mechanism different from that for the impaired secretion of exosomes from astrocytes.

Our findings suggest that exosomes are more likely to serve a protective function in the HD brains. We obtained several lines of evidence to support this idea. First, injection of exosomes into the HD KI mouse brain led to reduced HD-like neuropathology. Second, exosome secretion in the HD KI mouse brain decreased with mouse age and correlates with increased formation of mHtt aggregates. Third, mHtt inhibits αB-crystallin expression to reduce exosome secretion, whereas overexpression of αB-crystallin reverses this defect and its neuropathology. These findings are consistent with the emerging evidence that astrocyte-derived exosomes carrying neuroprotective cargo, such as heat shock proteins, contribute to neuronal survival (Taylor et al., 2007; Nafar et al., 2016). For example, exosomes derived from adipose-derived stem cells significantly decreased mHtt aggregates in cultured neuronal cells from R6/2 mice (Didiot et al., 2016; Lee et al., 2016; Lee et al., 2017). Because astrocytes from HD KI mice secrete less exosomes, the reduced secretion of exosomes from HD KI astrocytes may provide less protection to neurons in the HD mouse brains.

The fact that mHtt inhibits the expression of αB-crystallin to affect the release of exosomes from astrocytes is the most interesting finding from these studies. This defect is likely to contribute to HD neuropathology, as αB-crystallin plays a crucial role in several neurodegenerative disorders. For example, αB-crystallin can prevent amyloid fibril formation and reduces the toxicity of amyloid-β peptide in cells (Hochberg et al., 2014). αB-crystallin also inhibits the aggregation of α-synuclein fibrils in Parkinson's disease (Rekas et al., 2004; Waudby et al., 2010). The protective role of αB-crystallin in HD is also supported by the finding that expressing a mHtt fragment in the lens of mice lacking αB-crystallin markedly accelerated the onset and severity of mHtt aggregation (Muchowski et al., 2008). Decreased αB-crystallin levels were found in two HD mouse models, R6/2 and BACHD mice (Zabel et al., 2002; Oliveira et al., 2016), but the mechanism underlying this reduction remains uninvestigated. Our finding that mHtt reduces the expression of αB-crystallin to reduce exosome secretion is consistent with several known facts. First, αB-crystallin is mainly found in glial cells, but not neurons (Imura et al., 1999; Wyttenbach, 2004). Second, Sp1 regulates αB-crystallin transcription, whose function could be impaired by mHtt via abnormal protein interaction (Dunah et al., 2002; Li et al., 2002; Chen-Plotkin et al., 2006; Bradford et al., 2009). Third, only N-terminal Htt fragments accumulate in the nucleus, which can lead to gene transcription dysregulation and mHtt aggregations in an age-dependent manner. Consistently, we found that αB-crystallin also decreased in 10-month-old KI mice, in which N-terminal mHtt has obviously accumulated in the nuclei of striatal cells to form aggregates.

Because mHtt affects the secretion of astrocytic exosomes, this finding also offers new mechanistic insight into the HD pathology, especially the non–cell-autonomous neurotoxicity of mHtt. It is well known that mHtt preferentially affects the neurons in the striatum (Ross and Tabrizi, 2011; Bates et al., 2015). This preferential neurodegeneration likely results from different and multiple pathological pathways, including cell-autonomous or non–cell-autonomous disease processes (Ross and Tabrizi, 2011; Lee et al., 2013; Bates et al., 2015). Increasing evidence also indicates that mHtt affects multiple functions of glial cells to promote neurodegeneration (Hsiao and Chern, 2010; Lee et al., 2013). Of these adverse effects of mHtt in glial cells, transcriptional dysregulation appears to be a major mechanism for the toxic effect of mHtt in glial cells (Shin et al., 2005; Bradford et al., 2009; Tong et al., 2014; Huang et al., 2015). By examining exosomes released from astrocytes, we provide new evidence for the critical role of astrocytes in HD pathogenesis. Because mHtt is not found in the astrocytic exosomes, improving exosome secretion from astrocytes may be a potential, novel therapeutic strategy for HD.

References

Baker S, Polanco JC, Götz J (2016) Extracellular vesicles containing P301L mutant tau accelerate pathological tau phosphorylation and oligomer formation but do not seed mature neurofibrillary tangles in ALZ17 mice. J Alzheimers Dis 54:1207–1217. CrossRef Medline

Bates GP, Dorsey R, Gusella JF, Hayden MR, Kay C, Leavitt BR, Nance M, Ross CA, Scahill RI, Wetzel R, Wild EJ, Tabrizi SJ (2015) Huntington disease. Nat Rev Dis Primers 1:15005. CrossRef Medline

Bellingham SA, Guo BB, Coleman BM, Hill AF (2012) Exosomes: vehicles for the transfer of toxic proteins associated with neurodegenerative diseases? Front Physiol 3:124. CrossRef Medline

Bieri G, Gitler AD, Brahic M (2017) Internalization, axonal transport and release of fibrillar forms of alpha-synuclein. Neurobiol Dis. Advance online publication. Retrieved Mar. 16, 2017. CrossRef Medline

Bradford J, Shin JY, Roberts M, Wang CE, Li XJ, Li S (2009) Expression of mutant huntingtin in mouse brain astrocytes causes age-dependent neurological symptoms. Proc Natl Acad Sci U S A 106:22480–22485. CrossRef Medline

Caby MP, Lankar D, Vincendeau-Scherrer C, Raposo G, Bonnerot C (2005) Exosomal-like vesicles are present in human blood plasma. Int Immunol 17:879–887. CrossRef Medline

Chen-Plotkin AS, Sadri-Vakili G, Yohrling GJ, Braveman MW, Benn CL, Glajch KE, DiRocco DP, Farrell LA, Krainc D, Gines S, MacDonald ME, Cha JH (2006) Decreased association of the transcription factor Sp1 with genes downregulated in Huntington's disease. Neurobiol Dis 22: 233–241. CrossRef Medline

Coleman BM, Hill AF (2015) Extracellular vesicles: their role in the packaging and spread of misfolded proteins associated with neurodegenerative diseases. Semin Cell Dev Biol 40:89–96. CrossRef Medline

Colombo M, Raposo G, Théry C (2014) Biogenesis, secretion, and intercellular interactions of exosomes and other extracellular vesicles. Annu Rev Cell Dev Biol 30:255–289. CrossRef Medline

Costanzo M, Abounit S, Marzo L, Danckaert A, Chamoun Z, Roux P, Zurzolo C (2013) Transfer of polyglutamine aggregates in neuronal cells occurs in tunneling nanotubes. J Cell Sci 126:3678–3685. CrossRef Medline

Danzer KM, Kranich LR, Ruf WP, Cagsal-Getkin O, Winslow AR, Zhu L, Vanderburg CR, McLean PJ (2012) Exosomal cell-to-cell transmission of alpha synuclein oligomers. Mol Neurodegener 7:42. CrossRef Medline

Davies SW, Turmaine M, Cozens BA, DiFiglia M, Sharp AH, Ross CA, Scherzinger E, Wanker EE, Mangiarini L, Bates GP (1997) Formation of neuronal intranuclear inclusions underlies the neurological dysfunction in mice transgenic for the HD mutation. Cell 90:537–548. CrossRef Medline

Didiot MC, Hall LM, Coles AH, Haraszti RA, Godinho BM, Chase K, Sapp E, Ly S, Alterman JF, Hassler MR, Echeverria D, Raj L, Morrissey DV, DiFiglia M, Aronin N, Khvorova A (2016) Exosome-mediated delivery of hydrophobically modified siRNA for Huntingtin mRNA silencing. Mol Ther 24:1836–1847. CrossRef Medline

Dunah AW, Jeong H, Griffin A, Kim YM, Standaert DG, Hersch SM, Mouradian MM, Young AB, Tanese N, Krainc D (2002) Sp1 and TAFII130 transcriptional activity disrupted in early Huntington's disease. Science 296:2238–2243. CrossRef Medline

Gangalum RK, Bhat AM, Kohan SA, Bhat SP (2016) Inhibition of the expression of the small heat shock protein αB-crystallin inhibits exosome secretion in human retinal pigment epithelial cells in culture. J Biol Chem 291:12930–12942. CrossRef Medline

Gray M, Shirasaki DI, Cepeda C, André VM, Wilburn B, Lu XH, Tao J, Yamazaki I, Li SH, Sun YE, Li XJ, Levine MS, Yang XW (2008) Full-length human mutant huntingtin with a stable polyglutamine repeat can elicit progressive and selective neuropathogenesis in BACHD mice. J Neurosci 28:6182–6195. CrossRef Medline

Guitart K, Loers G, Buck F, Bork U, Schachner M, Kleene R. Guitart K, Loers G, Buck F, Bork U, Schachner M, Kleene R (2016) Improvement of neuronal cell survival by astrocyte-derived exosomes under hypoxic and ischemic conditions depends on prion protein. Glia 64:896–910. CrossRef Medline

Hajrasouliha AR, Jiang G, Lu Q, Lu H, Kaplan HJ, Zhang HG, Shao H (2013) Exosomes from retinal astrocytes contain antiangiogenic components that inhibit laser-induced choroidal neovascularization. J Biol Chem 288: 28058–28067. CrossRef Medline

Haney MJ, Zhao Y, Harrison EB, Mahajan V, Ahmed S, He Z, Suresh P, Hingtgen SD, Klyachko NL, Mosley RL, Gendelman HE, Kabanov AV, Batrakova EV (2013) Specific transfection of inflamed brain by macrophages: a new therapeutic strategy for neurodegenerative diseases. PLoS One 8:e61852. CrossRef Medline

Hickey MA, Kosmalska A, Enayati J, Cohen R, Zeitlin S, Levine MS, Chesselet MF (2008) Extensive early motor and non-motor behavioral deficits are followed by striatal neuronal loss in knock-in Huntington's disease mice. Neuroscience 157:280–295. CrossRef Medline

Hochberg GK, Ecroyd H, Liu C, Cox D, Cascio D, Sawaya MR, Collier MP, Stroud J, Carver JA, Baldwin AJ, Robinson CV, Eisenberg DS, Benesch JL, Laganowsky A (2014) The structured core domain of αB-crystallin can prevent amyloid fibrillation and associated toxicity. Proc Natl Acad Sci U S A 111:1562–1570. CrossRef Medline

Hong Y, Zhao T, Li XJ, Li S (2016) Mutant Huntingtin impairs BDNF release from astrocytes by disrupting conversion of Rab3a-GTP into Rab3a-GDP. J Neurosci 36:8790–8801. CrossRef Medline

Hsiao HY, Chern Y (2010) Targeting glial cells to elucidate the pathogenesis of Huntington's disease. Mol Neurobiol 41:248–255. CrossRef Medline

Huang B, Wei W, Wang G, Gaertig MA, Feng Y, Wang W, Li XJ, Li S (2015) Mutant huntingtin downregulates myelin regulatory factor-mediated myelin gene expression and affects mature oligodendrocytes. Neuron 85: 1212–1226. CrossRef Medline

Iguchi Y, Eid L, Parent M, Soucy G, Bareil C, Riku Y, Kawai K, Takagi S, Yoshida M, Katsuno M, Sobue G, Julien JP (2016) Exosome secretion is a key pathway for clearance of pathological TDP-43. Brain 139:3187–3201. CrossRef Medline

Iino M, Goto K, Kakegawa W, Okado H, Sudo M, Ishiuchi S, Miwa A, Takayasu Y, Saito I, Tsuzuki K, Ozawa S (2001) Glia-synapse interaction through Ca^{2+}-permeable AMPA receptors in Bergmann glia. Science 292:926–929. CrossRef Medline

Imura T, Shimohama S, Sato M, Nishikawa H, Madono K, Akaike A, Kimura J (1999) Differential expression of small heat shock proteins in reactive astrocytes after focal ischemia: possible role of beta-adrenergic receptor. J Neurosci 19:9768–9779. Medline

Jarmalavičiūtė A, Pivoriūnas A (2016) Exosomes as a potential novel therapeutic tools against neurodegenerative diseases. Pharmacol Res 113:816–822. CrossRef Medline

Jeon I, Cicchetti F, Cisbani G, Lee S, Li E, Bae J, Lee N, Li L, Im W, Kim M, Kim HS, Oh SH, Kim TA, Ko JJ, Aubé B, Oueslati A, Kim YJ, Song J (2016) Human-to-mouse prion-like propagation of mutant huntingtin protein. Acta Neuropathol 132:577–592. CrossRef Medline

Lee CY, Cantle JP, Yang XW (2013) Genetic manipulations of mutant Huntingtin in mice: new insights into HD pathogenesis. FEBS J 280:4382–4394. CrossRef Medline

Lee M, Liu T, Im W, Kim M (2016) Exosomes from adipose-derived stem cells ameliorate phenotype of Huntington's disease in vitro model. Eur J Neurosci 44:2114–2119. CrossRef Medline

Lee ST, Im W, Ban JJ, Lee M, Jung KH, Lee SK, Chu K, Kim M (2017) Exosome-based delivery of miR-124 in a Huntington's disease model. J Mov Disord 10:45–52. CrossRef Medline

Levy E (2017) Exosomes in the diseased brain: first insights from in vivo studies. Front Neurosci 11:142. CrossRef Medline

Li H, Li SH, Johnston H, Shelbourne PF, Li XJ (2000) Amino-terminal fragments of mutant huntingtin show selective accumulation in striatal neurons and synaptic toxicity. Nat Genet 25:385–389. CrossRef Medline

Li H, Li SH, Yu ZX, Shelbourne P, Li XJ (2001) Huntingtin aggregate-associated axonal degeneration is an early pathological event in Huntington's disease mice. J Neurosci 21:8473–8481. Medline

Li SH, Cheng AL, Zhou H, Lam S, Rao M, Li H, Li XJ (2002) Interaction of Huntington disease protein with transcriptional activator Sp1. Mol Cell Biol 22:1277–1287. CrossRef Medline

Maas SL, Breakefield XO, Weaver AM (2017) Extracellular vesicles: unique intercellular delivery vehicles. Trends Cell Biol 27:172–188. CrossRef Medline

Muchowski PJ, Ramsden R, Nguyen Q, Arnett EE, Greiling TM, Anderson SK, Clark JI (2008) Non-invasive measurement of protein aggregation by mutant huntingtin fragments or alpha-synuclein in the lens. J Biol Chem 283:6330–6336. CrossRef Medline

Nafar F, Williams JB, Mearow KM (2016) Astrocytes release HspB1 in response to amyloid-β exposure in vitro. J Alzheimers Dis 49:251–263. CrossRef Medline

Oliveira AO, Osmand A, Outeiro TF, Muchowski PJ, Finkbeiner S (2016) αB-Crystallin overexpression in astrocytes modulates the phenotype of the BACHD mouse model of Huntington's disease. Hum Mol Genet 25:1677–1689. CrossRef Medline

Pecho-Vrieseling E, Rieker C, Fuchs S, Bleckmann D, Esposito MS, Botta P, Goldstein C, Bernhard M, Galimberti I, Müller M, Lüthi A, Arber S, Bouwmeester T, van der Putten H, Di Giorgio FP (2014) Transneuronal propagation of mutant huntingtin contributes to non-cell autonomous pathology in neurons. Nat Neurosci 17:1064–1072. CrossRef Medline

Perez-Gonzalez R, Gauthier SA, Kumar A, Levy E (2012) The exosome secretory pathway transports amyloid precursor protein carboxyl-terminal fragments from the cell into the brain extracellular space. J Biol Chem 287:43108–43115. CrossRef Medline

Pisitkun T, Shen RF, Knepper MA (2004) Identification and proteomic profiling of exosomes in human urine. Proc Natl Acad Sci U S A 101:13368–13373. CrossRef Medline

Polanco JC, Scicluna BJ, Hill AF, Götz J (2016) Extracellular vesicles isolated from the brains of rTg4510 mice seed tau protein aggregation in a threshold-dependent manner. J Biol Chem 291:12445–12466. CrossRef Medline

Rekas A, Adda CG, Andrew Aquilina J, Barnham KJ, Sunde M, Galatis D, Williamson NA, Masters CL, Anders RF, Robinson CV, Cappai R, Carver JA (2004) Interaction of the molecular chaperone alphaB-crystallin with alpha-synuclein: effects on amyloid fibril formation and chaperone activity. J Mol Biol 340:1167–1183. CrossRef Medline

Ross CA, Tabrizi SJ (2011) Huntington's disease: from molecular pathogenesis to clinical treatment. Lancet Neurol 10:83–98. CrossRef Medline

Russo I, Bubacco L, Greggio E (2012) Exosomes-associated neurodegeneration and progression of Parkinson's disease. Am J Neurodegener Dis 1:217–225. Medline

Saudou F, Humbert S (2016) The biology of huntingtin. Neuron 89:910–926. CrossRef Medline

Schilling G, Becher MW, Sharp AH, Jinnah HA, Duan K, Kotzuk JA, Slunt HH, Ratovitski T, Cooper JK, Jenkins NA, Copeland NG, Price DL, Ross CA, Borchelt DR (1999) Intranuclear inclusions and neuritic aggregates in transgenic mice expressing a mutant N-terminal fragment of huntingtin. Hum Mol Genet 8:397–407. CrossRef Medline

Shin JY, Fang ZH, Yu ZX, Wang CE, Li SH, Li XJ (2005) Expression of mutant huntingtin in glial cells contributes to neuronal excitotoxicity. J Cell Biol 171:1001–1012. CrossRef Medline

Slow EJ, van Raamsdonk J, Rogers D, Coleman SH, Graham RK, Deng Y, Oh R, Bissada N, Hossain SM, Yang YZ, Li XJ, Simpson EM, Gutekunst CA, Leavitt BR, Hayden MR (2003) Selective striatal neuronal loss in a YAC128 mouse model of Huntington disease. Hum Mol Genet 12:1555–1567. CrossRef Medline

Swamynathan SK, Piatigorsky J (2007) Regulation of the mouse alphaB-crystallin and MKBP/HspB2 promoter activities by shared and gene specific intergenic elements: the importance of context dependency. Int J Dev Biol 51:689–700. CrossRef Medline

Takeuchi T, Suzuki M, Fujikake N, Popiel HA, Kikuchi H, Futaki S, Wada K, Nagai Y (2015) Intercellular chaperone transmission via exosomes contributes to maintenance of protein homeostasis at the organismal level. Proc Natl Acad Sci U S A 112:E2497–E2506. CrossRef Medline

Taylor AR, Robinson MB, Gifondorwa DJ, Tytell M, Milligan CE (2007) Regulation of heat shock protein 70 release in astrocytes: role of signaling kinases. Dev Neurobiol 67:1815–1829. CrossRef Medline

Théry C (2011) Exosomes: secreted vesicles and intercellular communications. F1000 Biol Rep 3:15. CrossRef Medline

Théry C, Zitvogel L, Amigorena S (2002) Exosomes: composition, biogenesis and function. Nat Rev Immunol 2:569–579. CrossRef Medline

Théry C, Amigorena S, Raposo G, Clayton A (2006) Isolation and characterization of exosomes from cell culture supernatants and biological fluids. Curr Protoc Cell Biol Chapter 3:Unit 3.22. CrossRef Medline

Tong X, Ao Y, Faas GC, Nwaobi SE, Xu J, Haustein MD, Anderson MA, Mody I, Olsen ML, Sofroniew MV, Khakh BS (2014) Astrocyte Kir4.1 ion channel deficits contribute to neuronal dysfunction in Huntington's disease model mice. Nat Neurosci 17:694–703. CrossRef Medline

Tydlacka S, Wang CE, Wang X, Li S, Li XJ (2008) Differential activities of the ubiquitin-proteasome system in neurons versus glia may account for the preferential accumulation of misfolded proteins in neurons. J Neurosci 28:13285–13295. CrossRef Medline

Vella LJ, Greenwood DL, Cappai R, Scheerlinck JP, Hill AF (2008) Enrichment of prion protein in exosomes derived from ovine cerebral spinal fluid. Vet Immunol Immunopathol 124:385–393. CrossRef Medline

Wang Y, Balaji V, Kaniyappan S, Krüger L, Irsen S, Tepper K, Chandupatla R, Maetzler W, Schneider A, Mandelkow E, Mandelkow EM (2017) The release and trans-synaptic transmission of Tau via exosomes. Mol Neurodegener 12:5. CrossRef Medline

Waudby CA, Knowles TP, Devlin GL, Skepper JN, Ecroyd H, Carver JA, Welland ME, Christodoulou J, Dobson CM, Meehan S (2010) The interaction of αB-crystallin with mature α-synuclein amyloid fibrils inhibits their elongation. Biophys J 98:843–851. CrossRef Medline

Westergard T, Jensen BK, Wen X, Cai J, Kropf E, Iacovitti L, Pasinelli P, Trotti D (2016) Cell-to-cell transmission of dipeptide repeat proteins linked to C9orf72-ALS/FTD. Cell Rep 17:645–652. CrossRef Medline

Wyttenbach A (2004) Role of heat shock proteins during polyglutamine neurodegeneration. J Mol Neurosci 23:69–95. CrossRef Medline

Xiao T, Zhang W, Jiao B, Pan CZ, Liu X, Shen L (2017) The role of exosomes in the pathogenesis of Alzheimer' disease. Transl Neurodegener 6:3. CrossRef Medline

Xin H, Wang F, Li Y, Lu QE, Cheung WL, Zhang Y, Zhang ZG, Chopp M (2017) Secondary release of exosomes from astrocytes contributes to the increase in neural plasticity and improvement of functional recovery after stroke in rats treated with exosomes harvested from microRNA 133b-overexpressing multipotent mesenchymal stromal cells. Cell Transplant 26:243–257. CrossRef Medline

Yu ZX, Li SH, Evans J, Pillarisetti A, Li H, Li XJ (2003) Mutant huntingtin causes context-dependent neurodegeneration in mice with Huntington's disease. J Neurosci 23:2193–2202.

Yue Q, Groszer M, Gil JS, Berk AJ, Messing A, Wu H, Liu X (2005) PTEN deletion in Bergmann glia leads to premature differentiation and affects laminar organization. Development 132:3281–3291. CrossRef Medline

Zabel C, Chamrad DC, Priller J, Woodman B, Meyer HE, Bates GP, Klose J (2002) Alterations in the mouse and human proteome caused by Huntington's disease. Mol Cell Proteomics 1:366–375. CrossRef Medline

Zhang X, Abels ER, Redzic JS, Margulis J, Finkbeiner S, Breakefield XO (2016) Potential transfer of polyglutamine and CAG-repeat RNA in extracellular vesicles in Huntington's disease: background and evaluation in cell culture. Cell Mol Neurobiol 36:459–470. CrossRef Medline

Zhao T, Hong Y, Li S, Li XJ (2016) Compartment-dependent degradation of mutant Huntingtin accounts for its preferential accumulation in neuronal processes. J Neurosci 36:8317–8328. CrossRef Medline

Zhao Y, Haney MJ, Gupta R, Bohnsack JP, He Z, Kabanov AV, Batrakova EV (2014) GDNF-transfected macrophages produce potent neuroprotective effects in Parkinson's disease mouse model. PLoS One 9:e106867. CrossRef Medline

Zheng T, Pu J, Chen Y, Mao Y, Guo Z, Pan H, Zhang L, Zhang H, Sun B, Zhang B (2017) Plasma exosomes spread and cluster around β-amyloid plaques in an animal model of Alzheimer's disease. Front Aging Neurosci 9:12. CrossRef Medline